Novel stable QTLs identification for berry quality traits based on high-density genetic linkage map construction in table grape

Huiling Wang
Beijing academy of agriclulture and forestry science
Ailing Yan
Beijing Academy of Agricultural and Forestry Sciences
Lei Sun
Beijing Academy of Agricultural and Forestry Sciences
Guojun Zhang
Beijing Academy of Agricultural and Forestry Sciences
Xiaoyue Wang
Beijing Academy of Agricultural and Forestry Sciences
Jiancheng Ren
Beijing Academy of Agricultural and Forestry Sciences
Haiying Xu (whlhappy@aliyun.com)
Beijing Academy of Agricultural and Forestry Sciences

Research article

Keywords: grapevine; high-density genetic linkage map; Muscat flavor; berry firmness; berry shape; candidate genes

Posted Date: April 28th, 2020

DOI: https://doi.org/10.21203/rs.3.rs-21147/v1

Version of Record: A version of this preprint was published on September 3rd, 2020. See the published version at https://doi.org/10.1186/s12870-020-02630-x.

Abstract

Backgroud: Aroma, berry firmness and berry shape are three main quality traits in table grape production, and also the important target traits in grapevine breeding. However, limited information about their genetic determinants leads to low accuracy and efficiency of quality breeding in grapevine. Mapping and isolation of quantitative trait locus (QTLs) based on the construction of genetic linkage map is a powerful approach to decipher the genetic determinants of complex quantitative traits in grape.

Results: In the present work, a final integrated map consisted of 6,436 SLAF markers on 19 linkage groups (LGs) spanning 3,365.41 cM in genome size with an average distance of 0.52 cM between adjacent markers was generated using the specific length amplified fragment sequencing (SLAF-seq) technique. Total 16 significant QTLs were identified on six linkage groups based on phenotypic data of Muscat flavor, berry firmness and berry shape among the hybrids analyzed over three consecutive years from 2016 to 2018. Notably, new QTLs for berry firmness and berry shape were found on LG 8 respectively for the first time, which had the strongest and most stable effects over 2-3 years. Based on biological function and expression profiles of candidate genes in the major QTL regions, 3 genes (*VIT_08s0007g00440*, *VIT_08s0040g02740* and *VIT_08s0040g02350*) related to berry firmness and 3 genes (*VIT_08s0032g01110*, *VIT_08s0032g01150* and *VIT_08s0105g00200*) linked to berry shape were highlighted. Overexpression of *VIT_08s0032g01110* in transgenic *Arabidopsis* plants caused the change of pod shape.

Conclusions: A new high-density genetic map with total 6634 markers was constructed with SLAF-seq technique, and thus enabled the detection of narrow interval QTLs for relevant traits in grapevine. *VIT_08s0007g00440*, *VIT_08s0040g02740* and *VIT_08s0040g02350* were found to be related to berry firmness, and *VIT_08s0032g01110*, *VIT_08s0032g01150* and *VIT_08s0105g00200* were linked to berry shape.

Background

Marker assisted selection (MAS) technology has been widely used to improve traditional breeding accuracy and efficiency in perennial crops [1]. One of the main objectives of grape breeding now is to develop molecular markers related to traits of interest for genetic selection of target phenotypes [2]. However, it needs to investigate the genetic determinisms for each given trait firstly. Quantitative trait loci (QTLs) mapping is one of the key and efficient approaches for dissecting complex traits in grapevine.

Numerous QTLs for grapevine relevant traits, such as berry weight and size [3–6], sweetness and acids [7–8], seedlessness [4–5, 9–10], disease-resistance traits [11–15], and so on, have been identified. In recent years, consumers pay more and more attention on grape quality, not only the taste traits (flavor, texture and so on) but also the appearance (color, berry size and shape). Promoting berry quality traits has been the endless pursuit of grapevine breeders. Muscat flavor, berry firmness and berry shape are

three main important quality traits in the breeding of new table grape varieties. The genetic determinants underlying their regulation have attracted extensive attention.

For Muscat flavor, a major QTL on linkage group (LG) 5 has been identified based on the phenotypic variation of the Muscat score analysis and evaluating monoterpenoid contents in three different F1 segregating progenies [16–18]. Because its colocalization with the major QTL positioned on chromosome 5, 1-deoxy-d-xylulose-5-phosphate synthase (*Vv*DXS) has been suggested as the candidate gene responsible for Muscat flavor [19]. Guo et al. [20] have also investigated that berry flavor was associated with chromosome 5, while the significant single nucleotide polymorphisms (SNP) associated with berry flavor was identified on *VIT_205s0020g03860* (homocysteine S-methyltransferase 2). Besides, some QTLs with smaller effects have been found on LG1, 7, 10 and 12 [16–18, 21]. Altogether, it can be seen that genetic control of Muscat flavor is complicated; more genetic studies on other hybrid populations grown in different environmental conditions would be needed.

Like most other grapevine agronomic traits, grape berry firmness also follows complex quantitative inheritance. That QTLs for grape berry firmness distributed on the different LGs has been investigated in different mapping populations. Carreño et al. [22] have firstly identified QTLs for berry firmness on LGs 1, 4, 5, 9, 10, 13, and 18 in 'Muscat Hamburg' × 'Sugraone' and 'Ruby Seedless' × 'Moscatuel'. In a progeny of 'Ruby Seedless' × 'Sultanina', the determinants for this trait are located on LG 8 and 18 [23]. While Ban et al. [24] have found two QTLs for firmness located on LGs 3 and 10 in a '*V. labruscana*'× '*V. vinifera*' cross. The most recent study has reported three QTLs all located on LG 18 in the progeny of 'Muscat Hamburg' and 'Crimson Seedless' [25]. However, most of the analyses have been performed using genetic linkage maps constructed with SSR markers, which resulted in the relatively large QTL confidence interval, and thus hinders the subsequent candidate genes identification.

For berry shape, to our knowledge, few studies have dealt with it in table grapes, although the diversity in berry shape is great for different grape cultivars. The wine grapes are generally round or nearly round. While, today's cultivated table grapes have diverse shapes, which can be divided into round, nearly round, broad ellipsoid, narrow ellipsoid, ovoid, obovoid, heart-shape, cylindric and so on. But the genetic determinism underlying this diversity is still unknown.

Genetic map construction is essential for the detection of QTLs associated with traits of agronomic interest. So far, a series of parental and consensus genetic maps have been developed by applying amplified fragment length polymorphism (AFLP) [26], sequence related amplified polymorphism (SRAP) [27], and single sequence repeat (SSR) [28–29] markers to different bi-parental segregating populations in grapevine. But majority of the genetic maps consist a limited number of markers with large map spacing and low resolution, thus are not able to provide precise and complete information about the numbers and locations of QTLs controlling the traits [30]. With the rapid development of the next generation sequencing (NGS) technology, genotyping through sequencing becomes the most direct and powerful method for the large-scale detection of SNP,which are considered as the markers of best choice for high-density genetic map construction [31–32]. At present, several high density genetic maps have

been constructed using NGS technologies, and some new QTLs have been successfully identified in grapevine [7, 11, 33–34]. There is no doubt that these high-density maps improve the efficiency and accuracy of QTL mapping, which can be used more effectively in breeding programs. However, QTL analysis for targeted traits mainly depends on the polymorphism between parents of the mapping populations. Lots of markers have distinct genotypes or linkage relationships in different hybrid populations [35]. So, it is necessary to develop new high density genetic linkage maps of grapevine for further QTL analysis of interest traits in grapevine.

Among all the NGS strategies, whole genome re-sequencing can identify whole genome wide differences between individuals and a large number of SNP markers [36]. But it is still too costly to apply in multiple samples, and generally unnecessary for linkage mapping. Specific length amplified fragment sequencing (SLAF-seq), a reduced representation sequencing approach, has been developed, which exhibits advantages in large-scale de novo SNP discovery and genotyping [37]. In the last 5 years, a series of high density genetic maps have been constructed based on SLAF-seq in diverse plant species [38–39]. Guo et al. [40] and Wang et al. [41] have successfully applied this method to construct high density genetic maps in grapevine too.

On these bases, in the present work, SLAF-seq was used in whole-genome genotyping for grapevine F1 lines; a consensus high-density genetic map was constructed with the developed SLAF markers. The map will facilitate the further precise identification of QTLs for major agronomic traits, and marker assisted selection in grape breeding programs. Moreover, the berry Muscat flavor, berry firmness and berry shape of F1 progenies and two parents were analyzed over 2–3 successive years. Quantitative trait loci (QTLs) for these three traits were identified and analyzed based on the consensus map. The candidate genes were predicted and validated by real time PCR. The results will broaden our understanding of the genetic control of these fruit traits, the tightly linked markers may be used to improve the fruit quality of grape.

Methods

Plant materials

The mapping population used in this study (line 1002; n = 160) was generated by crossing ‘Moldova’ (*V. vinifera* × *V. labruscana*) and ‘Ruidu Xiangyu’ (*V. vinifera*) [42] in 2010. The female parent ‘Ruidu Xiangyu’ was selected from a cross of ‘Jingxiu’ × ‘Xiangfei’ (Both are local varieties in china). ‘Ruidu Xiangyu’ is a grape with ovoid shape, greenish-yellow color, firm and crisp flesh and an excellent Muscat flavor. While the male parent ‘Moldova’ with ellipsoid shape, dark blue skin, soft flesh and neutral flavor, was derived from a cross of ‘Guzal Kara’ and ‘Villard blanc’. Moreover, ‘Moldova’ has high resistance to downy mildew and grey mold [43]. Altogether, there are great genetic differences between two parents, which supply excellent materials for high-density genetic map construction and subsequent QTL mapping. The plants of the two parents and their progeny were grown on their own roots in the experimental vineyard at Beijing academy of Forestry and Pomology (39°58’ N and 116°13’ E). The plants were spaced 1.0 m apart within the row and 2.5 m apart between rows, and rows were north-south oriented. They were maintained

under routine cultivation conditions, including soil management, fertilization, irrigation, pruning and disease control.

Phenotypic Measurements

Fully ripened berries (˚Brix ≥ 18) from F1 individuals and the two parents were collected in three successive seasons (2016–2018). Because of mechanical injury (In Beijing, the grape vine has to been buried underground to protect it from cold in winter), poor fruit setting, or bunch rot, not all F1 plants can set fruit or produce enough fruits for the later experiments. The number of harvested samples varied from year to year. In total, 115 genotypes were used in 2016, 133 in 2017, and 123 in 2018 for phenotypic measurement.

Muscat flavor was scored 0 (no flavor), 1 (light Muscat flavor), 3 (medium-level Muscat flavor) and 5 (strong Muscat flavor) independently by five tasters, each tasting at least three berries per offspring. The average score was used in further analysis.

Berry firmness was assessed over 2 years (2017–2018) according to the method of Carreño et al. [22] with universal TA. XTplus testing machine (Stable Micro Systems, Godalming, Surrey, UK). By using the device, firmness values were expressed as force (N) required for a 20% deformation of the berries. The average value of 20 berries per offspring was used in subsequent analysis.

The berry shape index (ShI) was determined as the ratio of the mean berry length (MBL) to the mean berry diameter (MBD). Berry length and diameter were assessed according to the OIV descriptors (OIV, 2009) with little modification. MBL was the mean value of 30 berries taken from the middle part of five representative clusters. MBD was the mean value of 30 berries taken from the middle part of five representative clusters. All measurements were taken with a hand caliper.

Statistical Analysis

The phenotypic data were analyzed using SPSS 13.0 software (SPSS, United States) to generate descriptive statistics, including the mean, minimum, maximum, standard deviation (SD), coefficient of variation (CV), skewness and kurtosis. The frequency distribution of phenotypic data was checked using Sigmaplot 10.0 software. The broad sense inheritability (H_b^2) was estimated following the methods of Liu et al. [44].

Dna Isolation

For DNA isolation, young and healthy leaves were harvested from each individual F1 plant and the two parents at the beginning of the vegetative period. The samples were immediately frozen in liquid nitrogen and stored in a − 70 °C freezer for further analysis.

DNA was extracted after grinding the samples to a fine powder with the Mixer-Mill-MM 300 grinder (Retsch, Haan, Germany) using the DNeasy plant mini prep kit (Qiagen). The DNA concentration was measured by a NanoDrop spectrophotometer (ND2000, Thermo Fisher Scientific, USA). The integrity of DNA was checked by gel electrophoresis.

Slaf Library Construction And Sequencing

SLAf-seq libraries were constructed as described by Sun et al. [37] with a small modification. In brief, a pilot SLAF experiment was performed to optimize conditions for obtaining maximum SLAF-seq efficiency. Based on the results, two enzymes, RsaI and HaeIII (New England Biolabs, USA), were used to digest the genomic DNA of each sample. After that, a single nucleotide (A) overhang was added to the purified digested fragments, and duplex tag-labeled sequencing adapters (PAGE-purified, Life Technologies, USA) were ligated to the A-tailed fragments. The PCR reaction was performed with diluted restriction-ligation DNA samples, dNTP, Taq DNA polymerase (NEB), and PCR primers. Then the PCR products were purified and pooled, and run on a 2% agarose gel. Fragments ranging from 400 to 450 bp (with indexes and adaptors) in size were isolated using a Gel Extraction Kit (Qiagen, Hilden, Germany). Gel-purified products were diluted, and pair-end sequencing (each end 150 bp) was performed on an Illumina HiSeq 2500 system (Illumina, Inc., San Diego, CA, USA). Real-time monitoring was performed for each cycle during sequencing, the ratio of high quality reads (quality score > 30) in the raw reads and GC content were calculated for quality control.

Sequencing Data Grouping And Genotyping

The procedures of sequencing data grouping and genotyping were performed as described previously [37]. Briefly, the Burrows-Wheeler Aligner (BWA) software was used to align clean reads from each sample against the *Vitis vinifera* reference genome (ftp://ftp.ensemblgenomes.org/pub/plants/release-25/fasta/vitis_vinifera/) with default parameters. Sequences mapped to the same position were defined as a single SLAF locus. Locus with two to four SLAF tags was identified as polymorphic SLAF. The average sequence depths of SLAF markers were greater than 20-fold in parents and greater than 8-fold in progeny. Polymorphic markers were classified into eight segregation patterns (ab × cd, ef × eg, hk × hk, lm × ll, nn × np, aa × bb, ab × cc and cc × ab). Based on the population type of F1, seven segregation patterns (excluding aa × bb) were selected for genetic map construction. In order to ensure the quality of the genetic map, three stringent filtering criteria were considered for the SLAF markers: i) with the average sequence depths of > 40-fold in the parents; ii) The number of SNP is < 8 per SLAF marker; iii) with less than 5% missing data. In addition, the chi-square test was then performed to examine the segregation distortion, and markers with significant segregation distortion ($P < 0.01$) were initially excluded from map construction.

Genetic Linkage Map Construction

Based on the locations on the grape genome, the filtered SLAF markers were partitioned into 19 linkage groups. The modified logarithm of odds (MLOD) scores between markers was calculated, and Markers with MLOD scores < 5 were filtered out before ordering. Highmap software was used to construct the genetic map of each linkage group as described by Liu et al. [45]. The error correction strategy of SMOOTH [46] was applied to correct genotyping errors, and a *k*-nearest neighbor algorithm [47] was used to impute genotyping missing. The enhanced algorithm of Gibbs sampling, spatial sampling and simulated annealing (GSS) [48–49] were employed to order markers. Map distances in centi-Morgans (cM) were calculated using the Kosambi mapping function [50]. For the construction of the consensus map, markers mapped in both parental maps and heterozygous markers (ab × ab) were used. Finally, the haplotype map, the heat map, and collinearity between the genetic and physical positions were analyzed by the method of Liu et al [45] to evaluate the quality of the constructed linkage map.

Qtl Mapping

Quantitative trait loci (QTLs) analysis for the berry Muscat flavor, berry firmness and berry shape were carried out on the consensus map using interval mapping with MapQTL 6.0 [51]. The threshold of LOD scores for evaluating the statistical significance of QTL effects was determined using 1,000 permutations. Based on these permutations, a LOD score of 3.0 was used as a minimum to declare the presence of a QTL in a particular genomic region. The genes within QTLs were identified by mapping the associated markers on the physical map. The genes were annotated and analyzed via the databases of Ensembl Plants (http://plants.ensembl.org/index.html) and NCBI (https://www.ncbi.nlm.nih.gov/). Possible candidate genes related to a specific trait were predicted based on their biological functions.

Validation Of Candidate Genes

To further validate the candidate genes related to each specific trait, grape berries of two parent cultivars, ‘Moldova’ and ‘Ruidu Xiangyu’, were sampled at young grape berry stage (stage A, pea-size berries), veraison (stage B, 50% berries turning red or soft), and fully ripening stage (stage C, ˚Brix ≥ 18) in 2018. The Muscat flavor, berry firmness, ShI and candidate gene expression of the sampled berries were analyzed too.

Total RNA was isolated from the different samples using a Plant RNA Isolation Kit (Sigma RT-50, St. Louis, MO, USA). The RNA integrity was verified using agarose gel electrophoresis. The first-strand complementary DNAs (cDNAs) were synthesized according to the manufacturer's instruction of AMV reverse transcriptase (Promega A3500). Then, two-step qPCR was carried out in the CFX 96 RT-PCR system (Bio-Rad, Richmond, CA) using a SYBR PCR kit (Tiangen, Beijing, China). The primers for all the candidate genes were designed by the Primer-Blast from NCBI (https://www.ncbi.nlm.nih.gov/tools/primerblast/) and their sequences are listed in Supplementary Table 1. Both *VvGAPDH* (CB975242) and *Vvubiquitin* (EC929411) were used as reference genes. The q-PCR reaction for each biological replicate was carried out in triplicate times.

Transformation of *in Arabidopsis*

The full-length cDNA of *VIT_08s0032g01110* were synthesized in the Beijing Sunbiotech Company (Beijing, China). The CDS of *VIT_08s0032g01110* was then fused to the downstream of CaMV35S promoter at the *Bgl II* (5' end)/ *BstE II* (3' end) sites by substitution of the GUS gene in pCAMBIA1301 vector. The *pCAMBIA1301:VIT_08s0032g01110* construct was introduced into *Agrobacterium tumefaciens* strain GV3101, which was used to infect Arabidopsis (ecotype Columbia-0) using the floral dip method. Positive transgenic Arabidopsis lines were screened by Hygromycin (Roche, Germany) and PCR to select T1 plants.

Results

Phenotypic data analysis

The phenotypic variation ranges of Muscat flavor (MF), berry firmness (BF) and berry shape index (ShI) for the two parents and the F1 progenies were presented in Supplementary Table 2 and Table 1. As the results shown, the berries of 'Ruidu Xiangyu' (female parent) with pronounced Muscat flavor showed a high Muscat flavor score. No Muscat flavor was tested in the berries of male parent 'Moldova'. In F1 population, the distribution for Muscat flavor score was continuous but highly skewed towards low values. Distributions of Muscat flavor score for each individual year are presented in skewed distribution as given in Fig. 1A.

Table 1
An overview of the phenopypic data of F1 population and two parents for each trait

Trait	Year	Ruidu Xiangyu (Female parent)	Moldova (Male parent)	Mid-Parent value	F1 population			
					Mean	**Range of variation**	**CV%**	Hb^2 **(%)**
MF	2016	4.00	0.00	2.00	0.86	0.00–5.00	118.02	70.98
	2017	4.25	0.00	2.13	0.55	0.00-4.50	158.07	58.85
	2018	4.20	0.00	2.10	0.47	0.00–5.00	196.08	65.18
BF (N)	2016	9.69	5.15	7.42	7.68	3.46–18.71	29.46	64.46
	2017	9.82	7.54	8.68	7.18	2.57–21.81	32.67	66.98
	2018	–	–	–	–	–	–	–
ShI	2016	1.12	1.24	1.12	1.19	1.02–1.45	7.09	61.91
	2017	1.00	1.18	1.00	1.16	0.83–1.44	8.05	69.32
	2018	1.03	1.26	1.03	1.15	0.92–1.44	7.79	66.32

Note: CV indicates coefficient of variation; H_b^2 represents the broad sense inheritability; MF is abbreviation of Muscat flavor; BF is abbreviation of berry firmness; ShI represents berry shape index.

Berry firmness was accessed in 2017 and 2018. The berries of ‘Ruidu Xiangyu’ and ‘Moldova’ showed medium and soft firmness, respectively, with mean force values of 9.69 and 5.15 N in 2017, and 9.82 and 7.54N in 2018. In their progenies, the average of BF in 2017 and 2018 ranged from 3.46 to 18.71, 2.57 and 21.81 N respectively, with a continuous distribution. Extreme phenotypes with higher or lower values than those of the parents were investigated, indicating transgressive segregation exited in the F1 progenies. The frequency distributions of BF over two years were shown in a normal distribution (Fig. 1B).

In terms of berry shape, the berries of ‘Ruidu Xiangyu’ were nearly rounded; ‘Moldova’ berries showed elliptical shape. Higher ShI value was observed in ‘Moldova’. The values of ShI in F1 population showed continuous variation, and transgressive distribution was observed (Fig. 1C). The F1 population mean value of ShI was 1.19 (2016), 1.16 (2017), and 1.15 (2018). The means of ShI in F1 population were over or equal to the mid-parent value in three successive years. Approximately similar normal phenotypic data distributions of ShI were examined for all three years (Fig. 1C).

As phenotypic data shown, all three traits showed quantitative inheritance, suggesting that they were controlled by multiple genes. However, high Broad-sense heritability (H_b^2) (more than 50%) was investigated for each trait (Table 1), which further indicated that there might be major QTLs affecting phenotypes.

Construction Of High Density Genetic Map

After SLAF library construction and high-throughput sequencing, a total of 310.67M paired-end reads were generated. The Q30 (a quality score of at least 30, indicating a 0.1% chance of an error, and thus 99.9% confidence) ratio was 88.97% and the average guanine-cytosine (GC) content was 39.57%. The reads were then mapped to the reference grapevine genome, a total of 263,676 high-quality SLAF tags were detected. The numbers of SLAFs in the male and female parents were 184,657 and 185,166, respectively. Among the detected 263,676 high-quality SLAF tags, 96,416 were polymorphic with a polymorphism ratio of 36.57%. Of these polymorphic SLAFs, 61,477 were classified into eight segregation patterns (Supplementary Figure. 1). Except for the aa × bb genotype, the other patterns were used for genetic map construction. After screening out the SLAF markers unsuitable for genetic map construction, a total of 6436 SLAF markers (3092 lm × ll, 2670 nn × np, 351 hk × hk, 290 ef × eg and 33 ab × cd) (Supplementary Table 3) were used for the final consensus high-density linkage map construction.

After linkage analysis, 6436 SLAF markers were clustered on 19 linkage groups (LG1-LG19), which were numbered according to the chromosome numbers (Fig. 2). As shown in Supplementary Table 4, there were 3766 SLAF markers in the paternal map of ‘Moldova’ (*V. vinifera* × *V. labruscana*) with total length 3342.75 cM. The average distance between adjacent markers was 0.56 cM. The length of each LG ranged from 135.7 cM (LG9) to 222.12 cM (LG10). LG15 contained only 58 SLAF markers with an average marker interval of 2.89 cM, whereas LG 14 contained the most markers (335) with an average marker interval length of 0.59 cM. The percentage of “Gap 5 cM” which reflected the degree of linkage between markers ranged from 82% (LG7) to 99% (LG19).

The maternal map of ‘Ruidu Xiangyu’ (*V. vinifera*) included 3344 SLAF markers. This map encompassed 3018.9 cM, with an average distance between adjacent markers of 0.91 cM. The largest LG was LG14 with 326 SLAF markers and an average interval length of 0.49 cM. The shortest LG17 contained only 76 markers with an average interval length of 1.39 cM. The percentage of the intervals between adjacent markers less than 5 cM ranged from 85–98% (Supplementary Table 5).

The consensus grape map included 6436 markers with a total genetic distance of 3365.41 cM (Table 2, Fig. 2 and Supplementary Fig. 2). The average interval distance between markers was 0.52 cM. The genetic length of the LGs ranged from 151.43 cM (LG4) to 199.44 cM (LG18). LG14 contained the highest number of markers (572), spanning 104.02 cM with the average genetic distance of 0.32 cM, whereas LG16 was the least saturated with the length of 151.43 cM and contained the lowest number of markers

(only 182). The percentage of “Gap < 5 cM” in each LG was more than 96% with the average value up to 98%.The largest gap was located in LG15 with 18.98 cM in length on this map.

Table 2
The information of the consencus high-density genetic map

Chr ID	Genome Size (Mb)	No of SLAFs	Distance (cM)	Average distance between markers (cM)	Collinearity %	Largest gap	Gap≤5 cM	Kb/cM
Chr1	25.31	411	199.22	0.49	98.41%	10.34	99%	127.04
Chr2	20.13	233	165.57	0.71	93.15%	17.83	98%	121.61
Chr3	22.05	254	192.96	0.76	89.52%	9.61	97%	114.25
Chr4	25.67	311	153.37	0.49	92.86%	18.74	99%	167.38
Chr5	27.28	355	149.4	0.42	97.99%	19.65	98%	182.58
Chr6	23.06	366	194.71	0.53	85.58%	9.75	99%	118.43
Chr7	24.09	357	179.96	0.51	87.14%	11.51	96%	133.89
Chr8	24.00	529	184.69	0.35	90.30%	15.06	97%	129.95
Chr9	25.19	364	188	0.52	95.45%	8.03	96%	133.98
Chr10	20.30	362	170.63	0.47	96.62%	11.69	99%	118.95
Chr11	21.55	264	164.15	0.62	96.16%	11.62	97%	131.29
Chr12	26.02	338	188.96	0.56	92.58%	15.48	97%	137.70
Chr13	29.66	357	199.44	0.56	82.63%	10.22	98%	148.72
Chr14	32.46	572	185.06	0.32	86.82%	10.26	98%	175.39
Chr15	21.77	195	170.59	0.88	92.34%	18.98	99%	127.61
Chr16	24.44	185	151.43	0.82	90.84%	16.57	99%	161.38
Chr17	19.25	192	171.6	0.9	97.05%	11.90	99%	112.19
Chr18	37.02	408	179.97	0.44	84.08%	7.40	99%	205.70
Chr19	25.75	383	175.7	0.46	96.27%	9.09	99%	146.58
Total	475.00	6,436	3,365.41	0.52	91.75%	/	98%	141.14

Evaluation Of The High-density Genetic Linkage Maps

The quality of the constructed genetic map is closely related to the accuracy of subsequent QTL mapping. Here, the sequence depths of SLAF markers on the map were analyzed firstly. As the results shown, the average sequencing depths of these 6436 markers were 56.12-fold for ‘Moldova’, 68.87-fold for ‘Ruidu Xiangyu’, and 16.71-fold for each individual progeny. The numbers of SLAF markers in each individual ranged from 5878 to 6434 with an average of 6366, and the sequencing depth ranged from 8.83-fold to 30.33-fold (Supplementary Fig. 3). These analysis results reflected the validity of molecular markers genotyping to a certain extent.

It is believed that haplotype and heat maps can directly reflect the quality of the genetic maps. Haplotype maps show recombination events in individuals, and heat maps reflect the recombination frequency and mapping location between markers. A haplotype map for LGs of the consensus map was shown in Supplementary Fig. 4. As the results shown, the occurrence of double crossovers and deletion ratio were low, indicating genotyping and marker-order of the LGs were accurate and reliable.

Heat maps were generated by using pair-wise recombination values for the 6436 mapped SLAF markers. The heat maps for the paternal map were also shown in Supplementary Fig. 5. The linkage between markers decreases with the increase of genetic distance, which indicates that the order of markers in the LGs is correct.

Furthermore, the colinearity between the genetic and physical positions on a linkage map was also analyzed. A relatively high level of genetic collinearity was observed between 19 LGs and the reference genome (Supplementary Fig. 6). As shown in Supplementary Table 6, the Spearman correlation coefficient ranged from 0.83 to 0.98, and it was higher than 0.90 in most LGs.

In general, from the results of haplotype maps, heat maps and colinearity analysis, the genetic maps constructed were of good performance for further QTL analysis.

Qtl Identification

QTL analyses were performed using the consensus genetic map. The QTLs detected for all the three traits are summarized in Table 3. A total of 16 QTLs were mapped on the consensus genetic map using the interval mapping method. Of the 16 QTLs, eight contributed to berry Muscat flavor, three were associated with fruit firmness, and the remaining five were related to berry shape.

Table 3
Summary of QTLs for three berry related traits over 3 successive years

Trait	QTL	Chr	Year of detection	Flanking Markers	Interval (cM)	Maximum LOD	PVE (%)
MF	qMF-1	5	2016	Marker2668298-Marker2755502	30.802–35.572	3.58	14.40
	qMF-2	5	2016	Marker2793749-Marker2740185	39.685–43.448	4.22	16.80
	qMF-3	17	2016	Marker64988-Marker142786	145.969-146.283	3.23	13.10
	qMF-4	5	2017	Marker2793749-Marker2847383	30.802–43.448	7.19	21.80
	qMF-5	5	2018	Marker2670960-Marker2847929	27.248–44.108	3.71	19.70
	qMF-6	1	2018	Marker2543100-Marker2576964	46.196–47.368	3.07	10.90
	qMF-7	7	2018	Marker2194644-Marker2378008	170.776-179.958	3.71	15.30
	qMF-8	18	2018	Marker406819-Marker419074	16.232–21.465	3.56	12.50
BF	qBF-1	1	2017	Marker2635745-Marker2622472	189.027-199.215	3.80	15.50
	qBF-2	8	2017	Marker1415166-Marker1507439	150.415-154.437	4.14	19.90
	qBF-3	8	2018	Marker1415166-Marker1409130	150.415-154.123	3.13	20.10
ShI	qShI-1	8	2016	Marker1415438-Marker1450563	2.565–8.655	5.74	20.50
	qShI-2	8	2017	Marker1415438-Marker1465950	2.565–5.097	6.5	20.80
	qShI-3	8	2017	Marker1399465	24.648	4.69	16.50
	qShI-4	8	2018	Marker1472237-Marker1416154	3.831–5.097	5.60	25.0
	qShI-5	8	2018	Marker1467244-Marker1413427	33.561–34.741	5.76	15.70

Note: Chr indicates chromosome; LOD indicates the logarithm of odds score; PVE indicates the phenotypic variance explained by individual QTL; MF is abbreviation of Muscat flavor; BF is abbreviation of berry firmness; ShI represents berry shape index.

Nine QTLs controlling Muscat flavor score were found on LG5, LG17, LG1, LG7 and LG18 in 3 successive years, respectively. The phenotypic variance explained by individual QTL (PVE) ranged from 10.90–21.80%. Among them, stable QTLs were detected on LG5 (qMF-1and qMF-2 in 2016; qMF-4 in 2017; qMF-5 in 2018). The four QTLs covered the same genetic interval (30.802–35.572 cM and 39.685–43.448 cM) respectively. The combined effect of the QTLs detected on LG5 in the same season explained up to 31.20% of the total phenotypic variance. In 2017, one additional QTL for Muscat flavor score was also detected on LG 17, which explained 13.10% of the total variance. In 2018, three other QTLs were mapped on LG1 (10.90% of PVE), LG7 (15.30% of PVE) and LG18 (12.50% of PVE), respectively.

Three significant QTLs kinked to berry firmness were located on LG1 (qBF-1) and LG8 (qBF-2 and qBF-3) respectively (Table 3). In 2017, two QTLs of berry firmness were identified. qBF-1 was mapped on LG1 explaining 15.50% of PVE with a peak LOD score of 3.8. qBF-2 was mapped on LG8 with a LOD score of 4.14 and an 19.90% of PVE. Only one QTL (qBF-3) was detected in 2018, which explained 20.10% of PVE. qBF-2 and qBF-3 shared the same genetic interval 150.415-154.123 cM. The position of the two QTL peaks was steady across the two seasons (Fig. 3A).

There were five QTL kinked to berry shape located on LG8, including qShI-1 (LOD = 5.74, 20.50% of PVE, 2016), qShI-2 (LOD = 6.5, 20.80% of PVE), qShI-3 (LOD = 4.69, 16.50% of PVE), qShI-4 (LOD = 5.60, 25.0% of PVE) and qShI-5 (LOD = 5.76, 15.70% of PVE). The QTLs of qShI-1, qShI-2 and qShI-4 covered the stable genetic interval (3.831–5.097 cM) between Marker1416154 and Marker1472237 in 3 successive years (Fig. 3B).

Candidate Genes Involved In Berry Quality Traits

Because stable genetic intervals were detected for each trait across years, the candidate genes located within these confidence intervals were henceforward being focused on. The linked markers in the confidence intervals were mapped on to the grapevine reference genome sequence. Four genomic regions of 2.90–4.11 Mb of chromosome 5 (related to Muscat flavor), 4.51–6.26 Mb of chromosome 5 (related to Muscat flavor), 13.44–15.71 Mb of chromosome 8 (linked to berry firmness), and 4.33–9.56 Mb of chromosome 8 (linked to berry shape index) were further analyzed. 157, 153, 244 and 141 genes in these regions were identified and annotated, respectively. Based on their biological function, 3, 6, 13 and 13 genes, respectively, were highlighted as good candidates for each trait (Supplementary Table 7). For Muscat flavor, a probable 1-deoxy-D-xylulose-5-phosphate synthase (*VIT_05s0020g02130*) was found in the region of 2.90–4.11 Mb of chromosome 5. *VIT_05s0020g03860* (a predicted homocysteine S-methyltransferase 3) was detected in 4.51–6.26 Mb of chromosome 5. A predicted expansin-A6 (*VIT_08s0007g00440*) and a probable pectate lyase 4 (*VIT_08s0040g02740*) were found in the region 13.44–15.71 Mb of chromosome 8 related to berry firmness. Additionally, *VIT_08s0032g01110* (predicted axial regulator YABBY 5) was included in the 13 good candidate genes related to the berry shape index.

Analysis of expressions of candidate genes during grape berry development

To further evaluate the potential relationship between candidate genes and each specific trait, the relative expression of corresponding candidate genes and berry related traits were analyzed during different grape berry development stages of two parent cultivars, ‘Moldova’ and ‘Ruidu Xiangyu’. As shown in Figure. 4A, berry firmness of ‘Moldova’ and ‘Ruidu Xiangyu’ both decreased at veraison. Thereafter, berry firmness of ‘Moldova’ still declined at the ripening stage, while that of ‘Ruidu Xiangyu’ increased significantly at the maturity stage (Fig. 4A). Among all the candidate genes (Supplementary Fig. 7A), the expression pattern of *VIT_08s0040g02350* was consistent with that of parents berry firmness, suggesting that *VIT_08s0040g02350* might associate with the variation of berry firmness in grape. There was an obvious increase in the expression of *VIT_08s0007g00440* in ‘Moldova’ at the ripening stage, but a significant decrease in ‘Ruidu Xiangyu’, which showed a contradictory pattern with the phenotypic variation.

The ShI of ‘Moldova’ and ‘Ruidu Xiangyu’ showed different change trends during berry development. Continuous reduction of ShI was observed in developing ‘Ruidu Xiangyu’, while ShI of ‘Moldova’ was firstly decreased but increased at the ripening stage. Among the analyzed genes, the relative expression of *VIT_08s0032g01110*, *VIT_08s0032g01150* and *VIT_08s0105g00200* showed a similar or opposite change patterns with that of ShI during berry development (Figure. 4B and Supplementary Fig. 7B). In particular, the expression level of *VIT_08s0032g01150* was increased gradually during grape berry development stage in ‘Ruidu Xiangyu’, but in ‘Moldova’ the relative expression of *VIT_08s0032g01150* were reduced at veraison and increased at ripening stage, which presented a completely opposite trends with the changes of ShI (Fig. 4B).

Unfortunately, among all the candidate genes studied, no genes were found consistent with the changes of Muscat flavor in both cultivars during berry development (Supplementary Fig. 7C).

Overexpression of *VIT_08s0032g01110* in Arabidopsis

Transgenic *Arabidopsis* plants overexpressing *VIT_08s0032g01110* were generated to elucidate its functions. As the results shown, differential pod shapes were observed between WT and *35S:VIT_08s0032g01110* seedlings (Fig. 5). The pods of *35S:VIT_08s0032g01110* plants showed curved, and their lengths were shorter than WT plants.

Discussion

Genetic map

The construction of a genetic map is very essential for mining the genetic basis of relevant traits, in particular of high-density genetic map construction, which will improve the efficiency and accuracy of further QTL analysis [30]. The important step in the construction of high-density maps is high-throughput discovery and genotyping of numerous molecular markers. The advent of NGS-based methods provides good opportunities for SNP markers development. Several high density genetic maps for grapevine have been constructed with NGS techniques [7, 11, 33–34, 40–41]. In the present work, a high-density genetic map for 'Moldova' × 'Ruidu Xiangyu' was constructed with SLAF-seq technique. The final integrated genetic linkage map consisted of 6433 SLAF markers on 19 LGs spanning a total genetic distance of 3365.41 cM, with an average distance of 0.52 cM between adjacent markers (Table 2 and Supplementary Fig. 2). Comparing to the previous reported maps constructed by the same SLAF-seq method [40–41], the number of markers in this study is lower, but it is still higher than other published high-density maps [7, 11, 33]. This difference may be related to the different F1 population used and different markers filtering parameters in genetic map construction [7]. In addition, the markers were distributed relative evenly on the whole genome (Fig. 2). The average distance between adjacent markers in all 19 LGs was less than 0.9 cM. The percentage of "Gap < 5 cM" reached up to 98% (Table 2). But it needs to point out that total length of the maps in this study were over 3000 cM, which is similar to that of maps constructed by Zhu et al [52], but longer than most other published maps [7, 11, 25, 33–34, 40–41]. Collard et al. [53] have suggested that the difference in chromosome recombination events occurred during sexual reproduction in each subpopulation can be the reason for the variation in map length. It also has been suggested that the very large map length may probably result from the low quality of markers or difficulty in ordering abundant markers in small populations with low recombination [54]. We were not sure about the reasons for the large length of the maps constructed in this work. However, stringent filtering criteria were considered for the SLAF markers in this study to ensure the marker quality. In the final, only 6436 markers from initial 96416 polymorphic SLAF markers were grouped on the map. The average sequencing depths of these 6436 markers were up to 68.87-fold for 'Ruidu Xiangyu', 56.12-fold for 'Moldova', and 16.71-fold for each individual progeny (Supplementary Fig. 3). Moreover, the low occurrence of double crossovers and deletion ratio were observed form haplotype maps (Supplementary Fig. 4), indicating genotyping and marker-order was reliable in the LG. The heat map of the marker exchange relationship was generated for evaluating the linkage relationship among the markers, suggesting that the recombination frequency and mapping location between markers was basically consistent in each LG (Supplementary Fig. 5). And a high level of genetic collinearity was observed between 19 LGs and the reference genome (Supplementary Fig. 6). Anyhow, the construction of this high density map for 'Moldova' × 'Ruidu Xiangyu' provides a key foundation for genetic analysis of many agronomic traits in grapevine.

Qtl Detection

The genetic factors for Muscat flavor have long been a concern of grape breeders. The researchers have identified a major QTL located on linkage group (LG) 5, and 1-deoxy-d-xylulose-5-phosphate synthase (*Vv*DXS) associated with the QTL has been considered as the candidate gene responsible for Muscat flavor [16–19]. In this work, total eight QTLs related to berry Muscat flavor were mapped on LG5, LG17,

LG1, LG7 and LG18 respectively cross 3 successive years based on sensory tasting data (Table 3). Similar to the previous results, major QTLs of qMF-1 and qMF-2 in 2016 (total 31.20% of PVE), qMF-4 in 2017(21.80% of PVE) and qMF-5 in 2018 (19.70% of PVE) were also identified located on LG5 in this mapping family. These QTLs shared the same genetic interval. It was noteworthy that compared with the previous single major QTL based on low-density maps, here two independent adjacent QTL loci (qMF-1: 30.802–35.572 cM and qMF-2: 39.685–43.448 cM) were identified respectively on LG5. And a probable DXS gene (*VIT_05s0020g02130*) was found in the genomic region of 30.802–35.572 cM (Supplementary Table 7), which is corresponding well to the previous finding [17]. While, *VIT_05s0020g03860* (a predicted homocysteine S-methyltransferase 3) was detected in the genomic region of 30.802–35.572 cM (Supplementary Table 7). Guo et al. [20] have investigated that one SNP on *VIT_205s0020g03860* was significantly associated with berry flavor. In addition, some other unstable QTLs (qMF-3 on LG17, qMF-6 on LG1, qMF-7 on LG7 and qMF-8 on LG18) were identified in 2016 and 2018 (Table 3). Previous studies have reported QTLs on LG1 and LG7 too, but also pointed out the limitation in minor QTLs detection using only Muscat score data [16]. Further QTL studies based on more detailed monoterpenes (the major contributors for Muscat flavor) components and contents will provide more information about genetic determinism for Muscat flavor.

The berry firmness of F1 progenies and parents was evaluated by the compression test, which has been suggested as a reliable method for providing information about the firmness of whole unpeeled berries [55]. Good correlations have been investigated between the quantitative data obtained from the texture analyzer and sensory parameters made by tasting [22]. In our experimental population, the phenotype of firmness showed continuous variation. The fluctuation was observed in firmness across years, suggesting the effect of environmental factors on this trait. But relatively high broad-sense heritability (H_b^2) of berry firmness was estimated reaching a value of 66.98% (Table 1), which were similar to the previous result (87.75% of H_b^2) obtained from ‘Ruby Seedless’ × ‘Sultanina’ progeny [23]. Based on the phenotypic data collected across two years, major QTLs qBF-2 (21.90% of PVE) and qBF-3 (20.10% of PVE) linked to berry firmness were detected on LG 8 (Table 3). Correa et al. [23] have also identified a stable QTL for berry firmness across seasons on LG 8 in a progeny of ‘Ruby Seedless’ × ‘Sultanina’. Interestingly, we found an expansin-A4 (*VIT_08s0007g00440)* located at 14,732,840–14,734,936 base pairs (bp) and a probable pectate lyase 4 (*VIT_08s0040g02740*) located at 13,772,697–13,781,967 bp in the genomic region of the two major QTLs (Supplementary Table 7). It has been suggested that expansins are involved in reassembly, degradation and expansion of cells and have a function in affecting berry softening in grape [56–58]. Pectate lyases have also been investigated to be related to grape berry texture [56, 59]. In addition, a minor effect QTL for berry firmness was mapped on LG 1 (Table 3), which is consistent with the previous report. Carreño et al. [22] have identified a QTL on LG 1 in two segregating progenies. However, we did not identify QTLs on LG18, which have been reported in other populations [22, 25]. This may be due to different genetic backgrounds and distinct phenotype evaluation methods [25].

Fruit shape is one of the vital appearance traits for horticulture crops. To date, various QTLs or candidate genes for fruit shape in different horticultural crops with fruits as their edible organs have been genetically confirmed [60–64]. However, few genetic studies have been focused on the identification of QTLs responsible for grape berry shape, although broad ranges of phenotypic variation in berry shape were observed in grape, especially in cultivated table grape. The grape berry shapes have always been intuitively classified by the traditional pictographic description, but it could not be directly used for QTL mapping analysis. Khambanonda. [65] has put forward the concept of "fruit shape index" to study the quantitative characters of pepper fruit. Fruit shape index can digitize the shape of fruit shape, which is more scientific than image description, and is more conducive to statistical analysis. Here, based on ShI data, 3 major QTLs (qShI-1, 20.50% of PVE; qShI-2, 20.80% of PVE and qShI-4, 25.0% of PVE) were identified on LG8 over 3 years. These three QTLs covered the same genetic interval (3.831–5.097 cM) (Table 3 and Fig. 3B). In the genomic region of the QTLs, *VIT_08s0032g01110* (predicted axial regulator YABBY 5) and a cluster of E3 ubiquitin-protein ligase (*VIT_08s0105g00180*, *VIT_08s0105g00190*, *VIT_08s0105g00200* and *VIT_08s0105g00290*) were identified (Supplementary Table 7), which might play an important function in grape berry shape formation. Previous evidences from tomato have suggested that the FASCIATED locus of six QTLs influencing tomato fruit shape is encoded by a member of the YABBY family [61]. While, Song et al. [66] have investigated a QTL for rice grain width encodes a previously unknown RING-type E3 ubiquitin ligase. It is suggested that homologous genes from different species may play similar biological functions [67].

Validation Of The Candidate Genes

We further investigated the expression profiles of several candidate genes in major QTL regions linked to three berry quality traits throughout berry development for two parent cultivars. For Muscat flavor, no gene expression patterns showed similar to the changes of Muscat flavor in two parent cultivars including DXS (Supplementary Fig. 7C), which has been suggested as the candidate gene responsible for Muscat flavor [19]. But this cannot exclude its role in Muscat flavor formation. Battilana et al. [68] have discovered the lysine with an asparagine at position 284 of the *Vv*DXS protein would affect Muscat flavor by influencing the enzyme catalytic efficiency. As to berry firmness, besides genes of an expansin-A4 (*VIT_08s0007g00440*) and a probable pectate lyase 4 (*VIT_08s0040g02740*), which families have been suggested playing important roles in fruit softening previously [56–59], the expression of an additional gene (*VIT_08s0040g02350*) was also consistent with the change of berry firmness, suggesting its role in affecting fruit firmness (Fig. 4A). Three candidate genes were highlighted for berry shape including *VIT_08s0032g01110*, *VIT_08s0032g01150* and *VIT_08s0105g00200*, the expression of which showed the similar or opposite change patterns with that of ShI during berry development (Fig. 4B). In particular, *VIT_08s0032g01110* was predicted as an axial regulator YABBY 5 gene. Its homologous gene *SlYABBY2* has been confirmed as one of major genetic factors regulating fruit shape in tomato [60], which *VIT_08s0032g01110* might play important regulatory role in grape berry shape formation. The transgenic Arabidopsis overexpressing *VIT_08s0032g01150* showed shorted and curved pod shape comparing to WT plants (Fig. 5).

Conclusions

In summary, a new high-density genetic map with total 6634 markers and an average distance of 0.52 cM between adjacent markers for 'Moldova' × 'Ruidu Xiangyu' was constructed with SLAF-seq technique, which provides a foundation for further genetic studies of relevant traits in grapevine. By using this map, 16 reliable QTLs linked to three grape berry quality traits were detected over 2–3 years, including 9 stable major QTLs. These QTL regions were significantly narrowed down compared to previous reports, which facilitated the subsequent candidate genes identification. The subsequent expression data of the candidate genes underlying the QTLs highlighted 3 genes related to berry firmness and 3 genes linked to berry shape respectively. Overexpression of *VIT_08s0032g01110* in transgenic Arabidopsis plants caused abrnomal pod shape. These results broaden our knowledge of the genetic control of these berry related traits and give bases for further functional and efficient DNA markers development for MAS in grapevine quality breeding.

Abbreviations

QTL: quantitative trait locus; LG: linkage group; SLAF: Specific length amplified fragment; MAS: marker assisted selection; DXS: 1-deoxy-d-xylulose-5-phosphate synthase; SNP: single nucleotide polymorphisms; AFLP: amplified fragment length polymorphism; SRAP: sequence related amplified polymorphism; SSR: single sequence repeat; NGS: next generation sequencing; ShI: berry shape index; MBL: mean berry length; MBD: mean berry diameter; H_b^2: broad sense inheritability; CV: coefficient of variation; MLOD: modified logarithm of odds; MF: Muscat flavor; BF: berry firmness; PVE: phenotypic variance explained by individual QTL.

Declarations

Ethics approval and consent to participate

This research was not applicable for ethics approval and consent to participate.

Consent for publication

This research is not applicable to consent for publication.

Competing interests

The authors declare no competing financial interests

Avalilability of data and materials

The *Vitis vinifera* reference genome referred in this work were downloaded from ftp://ftp.ensemblgenomes.org/pub/plants/release-25/fasta/vitis_vinifera/. The Phenotype data for Muscat flavor, berry firmness and berry shape in this work were presented in Supplementary Table 2. The

information of molecular markers used for map construction in this work was listed in Supplementary Table 3. The genes were annotated and analyzed via the databases of Ensembl Plants (http://plants.ensembl.org/index.html) and NCBI (https://www.ncbi.nlm.nih.gov/). The primers for qRT-PCR used in this research were designed by the Primer-Blast from NCBI (https://www.ncbi.nlm.nih.gov/tools/primerblast/) and their sequences are listed in Supplementary Table 1.

Author Contributions

Haiying Xu: Supervision, Conceptualization; Huiling Wang: Data curation, Writing- Original draft preparation; Huiling Wang, Ailing Yan, Lei Sun, Guojun Zhang, Xiaoyue Wang and Jiancheng Ren: Visualization, Investigation, Resources.

Funding

This research was supported by the National Natural Science Foundation of China (No. 31601712), Beijing Municipal Natural Science Foundation (No. 6182007), and the special fund of China Agriculture Research System (CARS-29).

References

1. van Nocker, S. & Gardiner, S. E. Breeding better cultivars, faster: applications of new technologies for the rapid deployment of superior horticultural tree crops. *Hortic Res*. **1**, 14022 (2014).
2. Yang, S. et al. A next-generation marker genotyping platform (AmpSeq) in heterozygous crops: a case study for marker-assisted selection in grapevine. *Hortic Res*. **3**, 16002 (2016).
3. Cabezas, J. A. A genetic analysis of seed and berry weight in grapevine. *Genome*. **49**, 1572–1585 (2006).
4. Doligez, A. et al. New stable QTLs for berry weight do not colocalize with QTLs for seed traits in cultivated grapevine (*Vitis vinifera* L.). *BMC Plant Biol*. **13**, 217 (2013).
5. Correa, J. et al. Quantitative trait loci for the response to gibberellic acid of berry size and seed mass in table grape (*Vitis vinifera* L.). *Aust J Grape Wine Res*. **21**, 496–507 (2015).
6. Zhao, Y. H. et al. Quantitative trait locus analysis of grape weight and soluble solid content. *Genet Mol Res*. **14**, 9872–9881 (2015).
7. Chen, J. Construction of a high-density genetic map and QTLs mapping for sugars and acids in grape berries. *BMC Plant Biol*. **15**, 14 (2015).
8. Bayo-Canha, A. et al. QTLs related to berry acidity identified in a wine grapevine population grown in warm weather. *Plant Mol Biol Rep*. **37**, 157–169 (2019).
9. Costantini, L. et al. Berry and phenology-related traits in grapevine (*Vitis vinifera* L.): From Quantitative Trait Loci to underlying genes. *BMC Plant Biol*. **8**, 38 (2008).

10. Royo, C. et al. The major origin of seedless grapes is associated with a missense mutation in the MADS-Box Gene*Vvi*AGL11. *Plant Physiol*. **177**, 1234–1253 (2018).
11. Sapkota, S. et al. Construction of a high-density linkage map and QTL detection of downy mildew resistance in *Vitis aestivalis*-derived 'Norton'. *Theor Appl Genet*. **132**, 137–147 (2019).
12. Pap, D. et al. Identification of two novel powdery mildew resistance loci, *Ren6* and *Ren7*, from the wild Chinese grape species *Vitis piasezkii*. *BMC Plant Biol*. **16**, 170 (2016).
13. Barba, P. et al. Two dominant loci determine resistance to Phomopsis cane lesions in F1 families of hybrid grapevines. *Theor Appl Genet*. **131**, 1173–1189 (2018).
14. Clark, M. D. Quantitative trait loci identified for foliar phylloxera resistance in a hybrid grape population. *Aust J Grape Wine Res*. **24**, 292–300 (2018).
15. Vezzulli, S. et al. The Rpv3-3 haplotype and stilbenoid induction mediate downy mildew resistance in a grapevine interspecific population. *Front Plant Sci*. **10**, 234 (2019).
16. Doligez, A., Audiot, E., Baumes, R. & This, P. QTLs for muscat flavor and monoterpenic odorant content in grapevine (*Vitis vinifera* L.). *Mol Breed*. **18**, 109–125 (2006b).
17. Battilana, J. et al. The 1-deoxy-d-xylulose 5-phosphate synthase gene co-localizes with a major QTL affecting monoterpene content in grapevine. *Theor Appl Genet*. **118**, 653–669 (2009).
18. Duchêne, E. et al. A grapevine (*Vitis vinifera* L.) deoxy-d-xylulose synthase gene colocates with a major quantitative trait loci for terpenol content. *Theor Appl Genet*. **118**, 541–552 (2009).
19. Emanuelli, F. et al. A candidate gene association study on muscat flavor in grapevine (Vitis vinifera L.). *BMC Plant Biol*. **10(1)**, 241 (2010).
20. Guo, D. L. et al. Genome-wide association study of berry-related traits in grape (*Vitis vinifera* L.) based on genotyping-by-sequencing markers. *Hortic Res*. **6**, 11 (2019).
21. Yang, X. X. et al. Genetic diversity and association study of aromatics in grapevine. *J Am Soc Hortic Sci*. **142**, 225–231 (2017).
22. Carreño, I. Quantitative genetic analysis of berry firmness in table grape (*Vitis vinifera* L.). *Tree Genet Genomes*. **11**, 818 (2015).
23. Correa, J. et al. New stable QTLs for berry firmness in table grapes. *Am J Enol Vitic*. **67**, 212–217 (2016).
24. Ban, Y. et al. Genetic dissection of quantitative trait loci for berry traits in interspecific hybrid grape (*Vitis labruscana* × *Vitis vinifera*). *Euphytica*. **211**, 295–310 (2016).
25. Jiang, J. F. et al. Construction of a high-density genetic map and mapping of firmness in grapes (*Vitis vinifera* L.) based on whole-genome resequencing. *Int J Mol Sci*. **21**, 797 (2020).
26. Doligez, A. et al. Genetic mapping of grapevine (*Vitis vinifera* L.) applied to the detection of QTLs for seedlessness and berry weight. *Theor Appl Genet*. **105**, 780–795 (2002).
27. Lodhi, M., Ye, G., Weeden, N., Reisch, B. & Daly, M. A molecular marker based linkage map of Vitis. *Genome*. **38**, 786–794 (1995).

28. Doligez, A. et al. An integrated SSR map of grapevine based on five mapping populations. *Theor Appl Genet*. **113**, 369–382 (2006a).
29. Schwander, F. et al. Rpv10: A new locus from the Asian Vitis gene pool for pyramiding downy mildew resistance loci in grapevine. *Theor Appl Genet*. **124**, 163–176 (2012).
30. Yu, H. H. Gains in QTL detection using an ultra-high density SNP map based on population sequencing relative to traditional RFLP/SSR markers. *PLoS One*. **6(3)**, e17595 (2011).
31. Wang, N. et al. Construction of a high-density genetic map for grape using next generation restriction-site associated DNA sequencing. *BMC Plant Biol*. **12**, 148 (2012).
32. Tello, J. et al. A novel high-density grapevine (*Vitis vinifera* L.) integrated linkage map using GBS in a half-diallel population. *Theor Appl Genet*. **132**, 2237–2252 (2019).
33. Fu, P. N. Cgr1, a ripe rot resistance QTL in *Vitis amurensis* 'Shuang Hong' grapevine. *Hortic Res*. **6**, 67 (2019).
34. Lewter, J. et al. High-density linkage maps and loci for berry color and flower sex in muscadine grape (*Vitis rotundifolia*). *Theor Appl Genet*. **132**, 1571–1585 (2019).
35. Khan, M.A. & Korban, S. S. Association mapping in forest trees and fruit crops. *J Exp Bot*. **63**, 4045–4060 (2012).
36. Xu, X. & Bai, G. Whole-genome resequencing: Changing the paradigms of SNP detection, molecular mapping and gene discovery. *Mol. Breed*. **35**, 1 (2015).
37. Sun, X. W. et al. SLAF-seq: an efficient method of large-scale denovo SNP discovery and genotyping using high-throughput sequencing. *PloS One*. **8(3)**, e58700 (2013).
38. Xu, W. W. et al. A high-density genetic map of cucumber derived from specific length amplified fragment sequencing (SLAF-seq). *Front Plant Sci*. **5**, 768 (2015).
39. Zhang, Z. et al. Construction of a high-density genetic map by specific locus amplified fragment sequencing (SLAF-seq) and its application to Quantitative Trait Loci (QTL) analysis for boll weight in upland cotton (*Gossypium hirsutum*.). *BMC Plant Biol*. **16**, 79 (2016).
40. Guo, Y. S. et al. Using specific length amplified fragment sequencing to construct the high-density genetic map for Vitis (*Vitis vinifera* L. x *Vitis amurensis* Rupr.). *Front Plant Sci*. **6**, 8 (2015).
41. Wang, J. H. et al. Construction of a high-density genetic map for grape using specific length amplified fragment (SLAF) sequencing. *PLoS one*. **12**, 17 (2017).
42. Xu, H.Y., Sun, L., Zhang, G. J. & Yan, A. L. 'Ruidu Xiangyu': A new table grape with Muscat flavor. *Vitis Geilweilerhof*. **51**, 143–144 (2012).
43. Maghradze, D., Mamasakhlisashvili, L. & Maul, E. Clarification of homonymy (misnaming) for a grapevine cultivar in Georgia: the case of 'Moldova' alias 'Aladasturi'. *Vitis Geilweilerhof*. **54**(Special issue), 73–76 (2015).
44. Liu, H. F. et al. Inheritance of sugars and acids in berries of grape (*Vitis vinifera* L.). *Euphytica*. 153, 99–107 (2007).

45. Liu, D. Y. Construction and analysis of high-density linkage map using high-throughput sequencing data. *PloS One*. 9(6), e98855 (2014).
46. van Os, H., Stam, P., Visser, R. G. & van Eck, H. J. SMOOTH: a statistical method for successful removal of genotyping errors from high-density genetic linkage data. *Theor Appl Genet*. **112**, 187–194 (2005).
47. Huang, X.H. et al. Genome-wide association study of flowering time and grain yield traits in a worldwide collection of rice germplasm. *Nat Genet*. **44(1)**, 32–39 (2011).
48. van Ooijen, J. Multipoint maximum likelihood mapping in a full-sib family of an outbreeding species. *Genet Res*. **93(5)**, 343–349 (2011).
49. Jansen, J., Jong, A. G. & Ooijen, J. W. Constructing dense genetic linkage maps. *Theor Appl Genet*. **102**, 1113–1122 (2001).
50. Kosambi, D. D. The estimation of map distances from recombination values. *Ann. Eugen*. **12**, 172–175 (1944).
51. Van Ooijen, J. W. MapQTL 6.0, Software for the mapping of quantitative trait loci in experimental populations of diploid species. Kyazma B.V., Wageningen, Netherlands. (2009)
52. Zhu, J. et al. Construction of a highly saturated genetic map for Vitis by next-generation restriction site-associated DNA sequencing. *BMC Plant Biol*. **18**, 347 (2018).
53. Collard, B. C. Y., Jahufer, M. Z. Z., Brouwer, J. B. & Pang, E. C. K. An introduction to markers, quantitative trait loci (QTL) mapping and marker-assisted selection for crop improvement: The basic concepts. *Euphytica*. **142**, 169–196 (2005).
54. Vezzulli, S., Doligez, A. & Bellin, D. Molecular Mapping of Grapevine Genes. In The Grape Genome (pp. 103-136). Springer, Cham (2019).
55. Rolle, L. et al. Instrumental texture analysis parameters as markers of table-grape and winegrape quality: a review. *Am J Enol Vitic*. **63**, 1 (2012).
56. Deluc, L.G. et al. Transcriptomic and metabolite analyses of bernet Sauvignon grape berry development. *BMC Genomics*. **8**, 429 (2007).
57. Schlosser, J. et al. Cellular expansion and gene expression in the developing grape (*Vitis vinifera* L.). *Protoplasma*. **232**, 255–265 (2008).
58. Dal Santo, S. et al. Genome-wide analysis of the expansin gene superfamily reveals grapevine-specific structural and functional characteristics. *PLoS One*. **8**, e62206 (2013).
59. Vargas, A. M. et al. Polymorphisms in *Vv*Pel associate with variation in berry texture and bunch size in the grapevine. *Aust J Grape Wine Res*. **19**, 193–207 (2013).
60. van der Knaap, E. et al. What lies beyond the eye: the molecular mechanisms regulating tomato fruit weight and shape. *Front Plant Sci*. **5**, 227 (2014).
61. Tan, J. Y. et al. A novel allele of monoecious (m) locus is responsible for elongated fruit shape and perfect flowers in cucumber (*Cucumis sativus* L). *Theor Appl Genet*. **128(12)**, 2483–2493 (2015).

62. Wu, S. et al. The control of tomato fruit elongation orchestrated by sun, ovate and fs8.1 in a wild relative of tomato. *Plant Sci*. **238**, 95–104 (2015).
63. Lopez-Girona, E. et al. A deletion affecting an LRR-RLK gene co-segregates with the fruit flat shape trait in peach. *Sci Rep*. **7(1)**, 6714 (2017).
64. Dou, J. L. et al. Genetic mapping reveals a candidate gene (ClFS1) for fruit shape in watermelon (*Citrullus lanatus* L.). *Theor Appl Genet*. **131(4)**, 947–958 (2018).
65. Khambanonda, I. Quantitative inheritance of fruit size in red pepper (*Capsicum frutescens* L.). *Genetics*. **35**, 322–343 (1950).
66. Song, X. J. et al. A QTL for rice grain width and weight encodes a previously unknown RING-type E3 ubiquitin ligase. *Nat Genet*. **39**, 623–630 (2007).
67. Monforte, A. J., Aurora, D., Caño-delgado, A. & van der Knaap, E. The genetic basis of fruit morphology in horticultural crops: lessons from tomato and melon. *J Exp Bot*. **65**, 4625–4637 (2014).
68. Battilana, J. et al. Functional effect of grapevine 1-deoxy-D-xylulose 5-phosphate synthase substitution K284N on Muscat flavour formation. *J Exp Bot*. **62(15)**, 5497–5508 (2011).

Supplementary Figure Legends

Supplementary Figure legends

Supplementary Figure 1. Number of markers in each of eight segregation patterns.

Supplementary Figure 2. The consensus genetic linkage map generated using 160 hybrid seedlings derived from ‘Moldova’ × ‘Ruidu Xiangyu’.

Supplementary Figure 3. The average sequencing depths of markers on the consensus map in F1 population. The x-axis indicates individual F1 plant accessions; the y-axis indicates the average depths.

Supplementary Figure 4. Haplotype maps of the consensus genetic map. Green represents ‘Moldova’, blue represents ‘Ruidu Xiangyu’, gray represents missing data, and white indicates heterozygosity. Each two columns represent the genotype of an individual. Rows correspond to genetic markers.

Supplementary Figure 5. Heat maps of the paternal genetic map. Each cell represents the recombination rate of two markers. Yellow indicates a lower recombination rate and purple a higher one.

Supplementary Figure 6. Correlation of the genetic and physical positions. The x-axis represents the genetic groups; the y-axis represents the physical positions.

Supplementary Figure 7. Heatmaps of berry firmness (BF), berry shape index (ShI), Muscat flavor (MF) and the expressions of candidate genes during grape berry development in ‘Moldova’ and ‘Ruidu Xiangyu’. (A) Expressions of all the filtered candidate genes for berry firmness. (B) Expressions of the

filtered candidate genes for berry shape. (C) Expressions of candidate genes for berry Muscat flavor. Dark blue indicates a lower level and red a higher level.

Figures

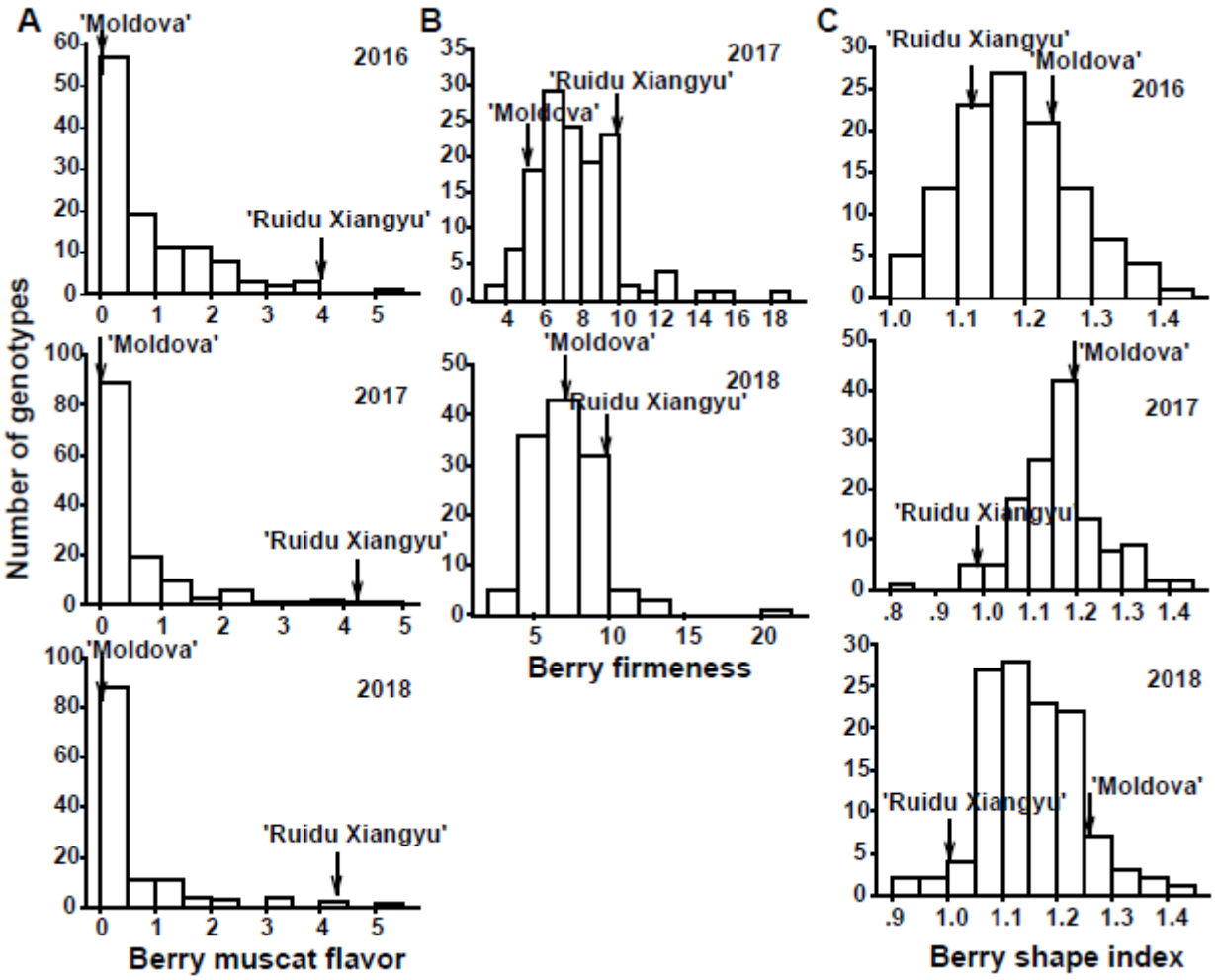

Figure 1

Genetic map lengths and marker distribution in 19 linkage groups of the consensus map. Genetic distance is indicated by the vertical scale in centi-Morgans (cM). Black lines represent mapped markers. 1-19 represent corresponding linkage groups ID.

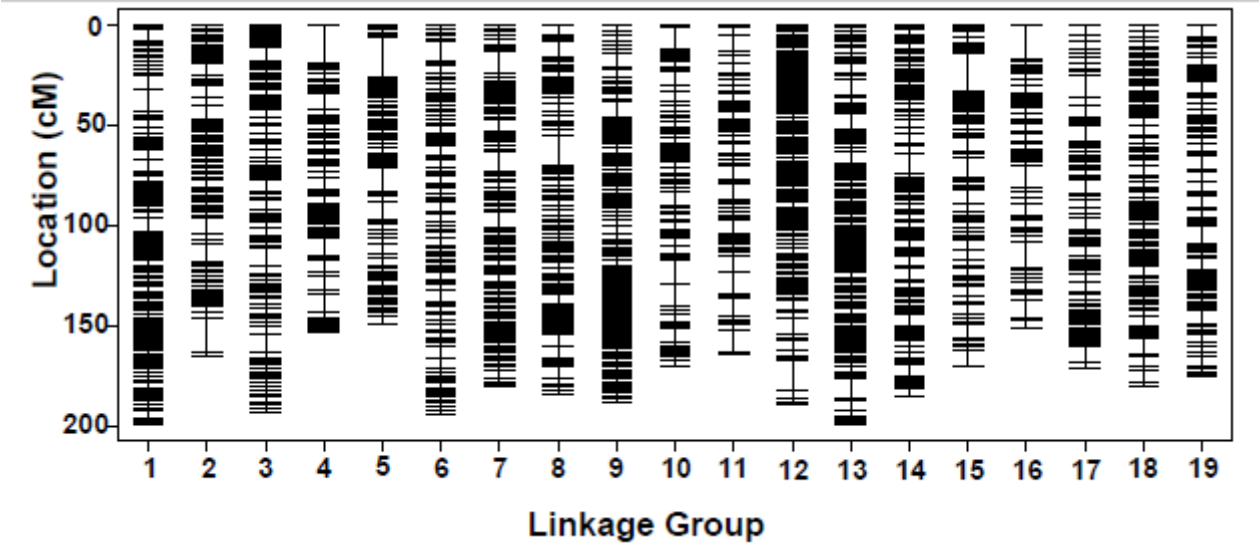

Figure 2

Phenotypic distribution of Muscat flavor (A), berry firmness (B) and Berry shape index (C) over 2-3 years for ‘Moldova’ × ‘Ruidu Xiangyu’ progeny. The plot was based on mean values of each genotype. The parental mean values are indicated by their names.

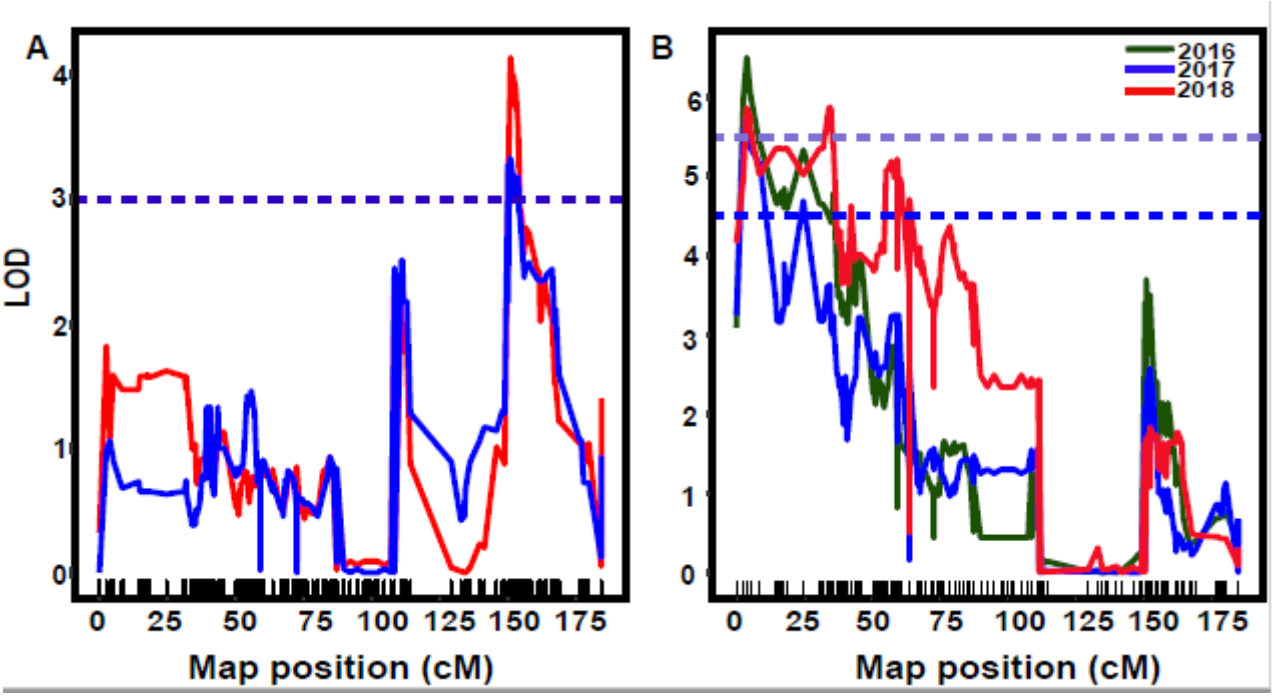

Figure 3

Precise locations of major QTLs for berry firmness and berry shape in the consensus map. (A) LOD curves of QTL mapping for berry firmness on chromosome 8 in 2017-2018. (B) LOD curves of QTL mapping for berry shape index on chromosome 8 in 3 successive years. Short lines on x-axis indicate the genetic positions of the SLAF markers.

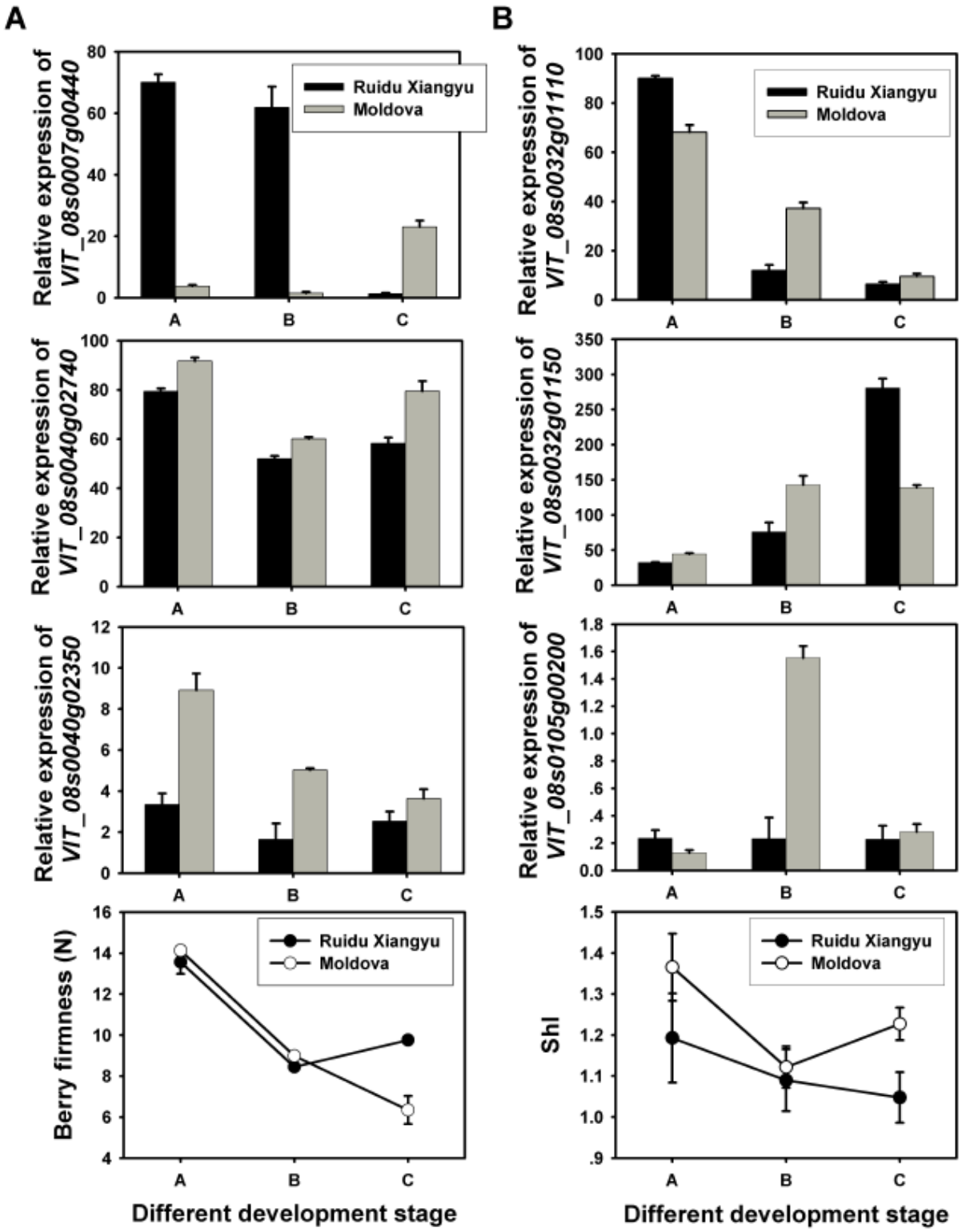

Figure 4

The Changes of berry firmness, berry shape index and expressions of candidate genes during grape berry development in ‘Moldova’ and ‘Ruidu Xiangyu’. (A) Expressions of three filtered candidate genes for berry firmness. (B) Expressions of three candidate genes for berry shape.

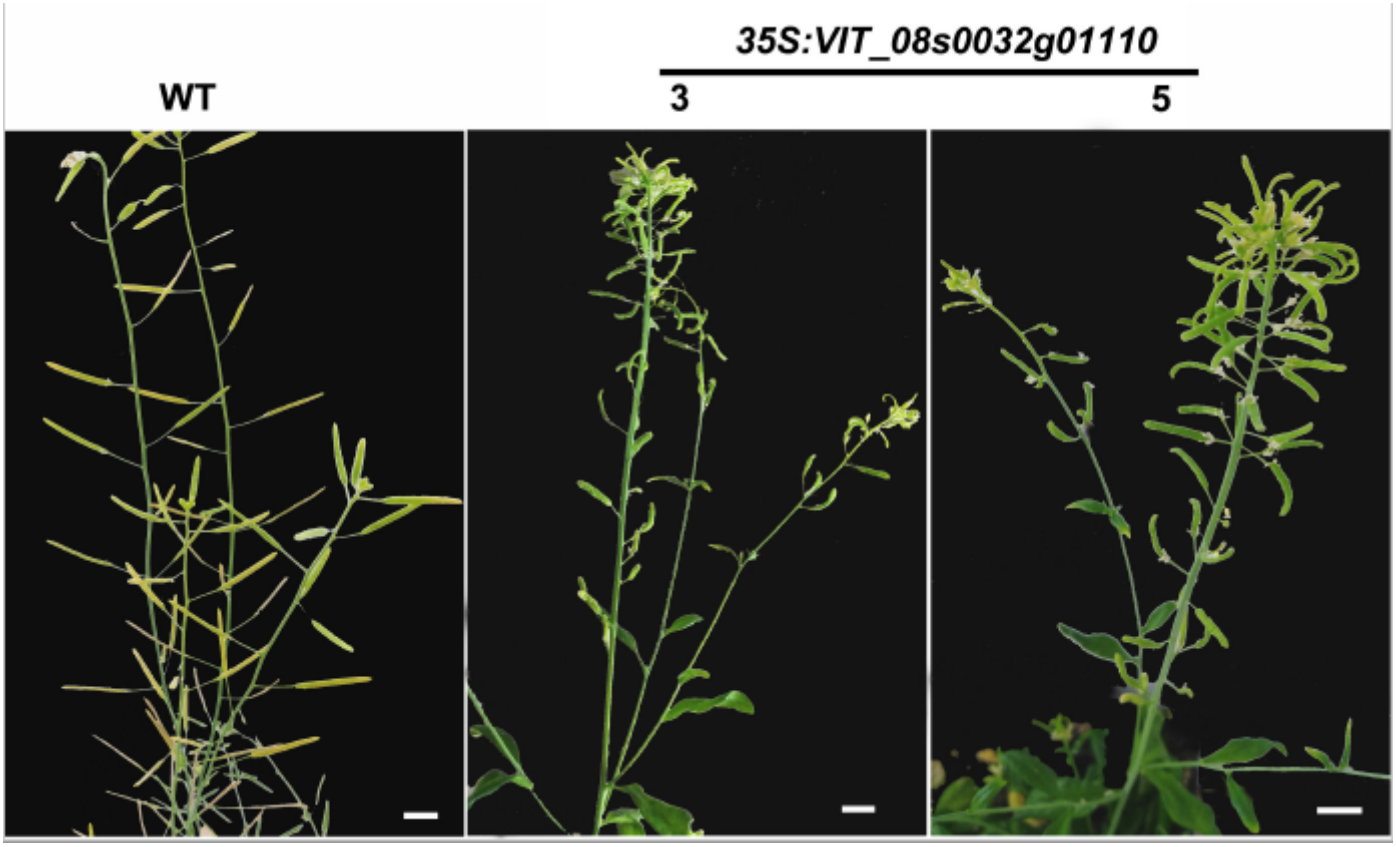

Figure 5

Pod shapes in 35S:VIT08s0032g01110 and WT Arabidopsis plants. Scale bar, 4 mm.

Supplementary Files

This is a list of supplementary files associated with this preprint. Click to download.

- Supplementaryfigure1.pdf
- SupplementaryTable146.docx
- SupplementaryTable2.xlsx
- SupplementaryTable7.xlsx
- SupplementaryTable3.xlsx
- Supplementaryfigure5.pdf
- Supplementaryfigure3.pdf
- SupplementaryFigure7.pdf
- Supplementaryfigure2.pdf
- SupplementaryFigure6.pdf
- Supplementaryfigure4.pdf